

1

2 Characterising *RAG1* and *RAG2* with predictive genomics

3 Dylan Lawless, MSc^{a,*}, Jolan E. Walter, MD, PhD^{b,c}, Rashida Anwar, PhD^a,
4 Sinisa Savic, MD, PhD^{d,e,*}

5 ^a*Leeds Institute of Biomedical and Clinical Sciences, University of Leeds, Wellcome Trust*
6 *Brenner Building, St James's University Hospital, Beckett Street, Leeds, UK.*

7 ^b*University of South Florida and Johns Hopkins All Children's Hospital, Saint Petersburg, FL, USA.*

8 ^c*Division of Allergy Immunology, Massachusetts General Hospital for Children, Boston, MA, USA.*

9 ^d*Department of Clinical Immunology and Allergy, St James's University Hospital, Beckett Street, Leeds, UK.*

10 ^e*National Institute for Health Research Leeds Musculoskeletal Biomedical Research Centre and*
11 *Leeds Institute of Rheumatic and Musculoskeletal Medicine, Wellcome Trust Brenner Building,*
12 *St James's University Hospital, Beckett Street, Leeds, UK.*

13 Abstract

While widespread genome sequencing ushers in a new era of preventive medicine, the tools for predictive genomics are still lacking. The greatest hurdle in diagnosis of rare disease is validation for variants of unknown significance. RAG deficiency presents at an early age with a distinct phenotype of combined immunodeficiency with granuloma and/or autoimmunity. Allele frequency of a SNV in the general population is an indicator of the functional or structural importance of a particular amino acid residue. However, rare diseases are often attributable to variants in genes which are highly conserved. Mutation of a conserved residue does not confirm pathogenicity and functional validation must be confirmed to correctly identify a monogenic disorders such as RAG deficiency. We present protein variants in RAG1 and RAG2 which are most likely to be seen clinically as disease-causing. Our method of mutation rate residue fre-

*Addresses for correspondence

Email addresses: D.Lawless@leeds.ac.uk (Dylan Lawless, MSc),
S.Savic@leeds.ac.uk (Sinisa Savic, MD, PhD)

quency builds a map of most probable mutations allowing pre-emptive functional analysis. We compare the accuracy of our predicted probabilities to previously established functional measurements.

14 **Acknowledgements**

15 This work is funded by the University of Leeds 110 Anniversary Research Schol-
16 arship. Dr. Jolan Walter has received federal funding. The authors declare no
17 conflict of interest.

18 **Key words**

19 RAG1, RAG2, genomics.

20 **Abbreviations**

21 CADD (combined annotation dependent depletion), GWAS (genome-wide as-
22 sociation studies), M_r (mutation rate), MFR (mutation rate residue frequency),
23 (pLI) probability of being loss-of-function intolerant, R_f (residue frequency),
24 RAG1 (recombination activating gene 1).

25

26 **Introduction**

27 Costs associated with genomic investigations continue to reduce [1] while the
28 richness of data generated increases. Globally, the adoption of wide scale genome
29 sequencing implies that all new-born infants may receive screening for pathogenic
30 genetic mutation in an asymptomatic stage, pre-emptively [2]. The one di-
31 mensionality of individual genomes is now being expanded by the possibility
32 of massive parallel sequencing for somatic variant analysis and by single-cell
33 or lineage-specific genotyping; culminating in a genotype spectrum. In whole
34 blood, virtually every nucleotide position may be mutated across 10^5 cells [3].
35 Mapping one's genotype across multiple cell types and at several periods dur-
36 ing a person's life may soon be feasible [4]. Such genotype snapshots might
37 allow for prediction and tracking of somatic, epigenetic, and transcriptomic
38 profiling.

39 The predictive value of the screening highly depends on the computation
40 tools used for data analysis and its correlation with functional assays or prior
41 clinical experience. Interpretation of that data is especially challenging for vari-
42 ants of unknown significance. There is a need for predictive genomic modelling
43 with aims to provide a reliable guidance for therapeutic intervention for pa-
44 tients harbouring genetic defects for life threatening disease before the illness
45 becomes clinically significant. Although, most genomic investigations currently
46 are not predictive for clinical outcome. The study of predictive genomics is ex-
47 emplified by consideration of gene essentiality, accomplished by observing in-
48 tolerance to loss-of-function variants. Several gene essentiality scoring meth-

49 ods are available for both the coding and non-coding genome [5]. Approxi-
50 mately 3,000 human genes cannot tolerate the loss of one allele [5]. The great-
51 est hurdle in monogenic disease is the interpretation of variants of unknown
52 significance while functional validation is a major time and cost investment
53 for laboratories investigating rare disease. Severe, life-threatening immune dis-
54 eases are caused by genetic variations in almost 300 genes [6, 7] however, only
55 a small percentage of disease causing variants have been characterised with
56 functional studies. Our investigation aims to apply predictive genomics as a
57 tool to identify pathogenic genetic variants that are most likely to be seen in
58 patient cohorts.

59 We present the first application of our novel approach of predictive genomics
60 using Recombination activating gene 1 (*RAG1*) and *RAG2* deficiency as a model
61 for a rare primary immunodeficiency caused by autosomal recessive variants.
62 *RAG1* and *RAG2* encode lymphoid-specific proteins that are essential for V(D)J
63 recombination. This genetic recombination mechanism is essential for a ro-
64 bust immune response by diversification the T and B cell repertoire in the thy-
65 mus and bone marrow, respectively [8, 9]. *RAG* deficiency is measured by in
66 vitro quantification of recombination activity. Hypomorphic *RAG1* and *RAG2*
67 mutations with residual V(D)J recombination activity (in average 5-30%) re-
68 sult in a distinct phenotype of combined immunodeficiency with granuloma
69 and/or autoimmunity (CID-G/A) [2, 10, 11]. *RAG1* and *RAG2* are highly con-
70 served genes but disease is only reported with autosomal recessive inheritance.
71 Only 44% of amino acids in *RAG1* and *RAG2* are reported as mutated on Gno-
72 mAD and functional validation of clinically relevant variants is difficult. Pre-

73 empty selection of residues for functional validation is a major challenge; a
74 selection based on low allele frequency alone is infeasible. A shortened time be-
75 tween genetic analysis and diagnosis means that treatments may be delivered
76 earlier. With such tools, patients with RAG deficiency may receive hemato poi-
77 etic stem cell transplant [12] or be provided mechanism-based treatment [13].

78 GnomAD was queried to identify conserved residues using a Boolean score
79 C (0 or 1, although allele frequency can be substituted). The gene-specific mu-
80 tation rate M_r of each residue was calculated from allele frequencies. The gene-
81 specific residue frequency R_f was also calculated and together the values calcu-
82 late the most probable disease-causing variants which have not yet been iden-
83 tified in patients. We term the resulting score a mutation rate residue frequency
84 (MRF); where $MRF = C \times M_r \times R_f$. For visualisation, a noise reduction method
85 was also applied where the average MRF per 1% interval is displayed with a
86 cut-off threshold at the 75th percentile.

87 **Results**

88 *RAG1 and RAG2 conservation and mutation rate residue frequency.*

89 Fig 1 presents the most probable unidentified disease-causing variants in RAG1/2.
90 Phenotypic, epigenetic, or other such weighting data may also be applied to
91 this model. Variants with a low MRF may still be damaging but resources for
92 functional validation are best spent on gene regions with high MRF. Clusters
93 of conserved residues are shown in Fig 1(i) however; these clusters do not pre-
94 dict the likelihood of clinical presentation. Raw MRF scores are presented in
95 Fig 1(ii). A histogram illustrates the MRF without Boolean scoring applied and

96 Fig 1(iii) presents a clearer visualisation. Table S1 provides all MRF scores for
97 both proteins as well as raw data used for calculations and the list of validated
98 residues of RAG1 and RAG2.

99 *MRF score versus known variant pathogenicity measure*

100 The functional validation of these predictions is presented in Fig 1(v). We have
101 previously measured the recombination activity of RAG1 and RAG2 disease-
102 causing variants in several patients [14]. We have combined the known func-
103 tional activity from other extensive reports [15], to compare a total of 44 vari-
104 ants. RAG deficiency is measured by the level of recombination potential. We
105 expected that damaging mutations (resulting in low recombination activity in
106 vitro) would be identified with high MRF scores. MRF pathogenicity prediction
107 correctly identified damaging mutations in RAG1 and RAG2 (Fig 1(v)). Variants
108 reported on GnomAD which are clinically found to cause disease have signifi-
109 cantly higher MRF scores than variants which have not been reported to cause
110 disease (Fig 1(v)). Table S1 provides all MRF scores for both proteins as well as
111 raw data used for calculations and the list of validated residues of RAG1 and
112 RAG2.

113 Allele frequency is generally the single most important filtering method for
114 rare disease in whole genome (and exome) sequencing experiments. *RAG1* and
115 *RAG2* have probability of being loss-of-function intolerant (pLI) scores of 0.00
116 and 0.01, respectively. Mutations under pressure from purifying selection are
117 more likely to cause disease than common variants. However, allele frequen-
118 cies of rare variants reported on GnomAD cannot differentially predict likeli-

119 hood of causing disease. This is particularly important for recessive diseases
120 such as RAG deficiency. As such we find no significant difference between clini-
121 cally damaging variants and those which have not been reported yet as disease-
122 causing, illustrating the reasoning for our method design (Fig 1 (vi)). Many
123 non-clinically-reported rare variants may cause disease; the MRF score identi-
124 fies the top clinically-relevant candidates. Conserved residues with the highest
125 MRF for both RAG1 and RAG2 are mapped onto the protein structure in Fig 3
126 and frequently show high MRF at DNA contact points. The accuracy for cor-
127 rectly identifying all disease-causing variants reported to date is shown in (Fig
128 1(vii)). We found >80% accuracy for 21 known variants tested, >50% accuracy
129 for 48 tested and <50% accuracy for only 23 tested. The raw values comparing
130 functional pathogenicity and MRF scores are illustrated in Fig 2.

131 *False positives in Transib domains do not worsen probability prediction*

132 A set of conserved motifs in core *RAG1* are shared with the *Transib* transposase,
133 including the critical DDE residue catalytic triad [16]. Ten *RAG1* core motifs are
134 conserved amongst a set of diverse species including human [16]. To assess the
135 influence of false positive effect on MRF prediction the conserved residues in
136 this dataset are compared to GnomAD allele frequencies and MRF score. Fig 4
137 (i) plots the MRF (lacking the Boolean component *C*) for conserved *Transib* mo-
138 tif residues, non-conserved *Transib* motif residues, and non-*Transib* residues.
139 Fig 4 (ii) shows the percentage of these which are reported as mutated on Gno-
140 mAD. Removing reported variants by applying *C*, the resulting effect on incor-
141 rectly scoring MRF in the conserved *Transib* motifs remains neutral. Com-

142 bined Annotation Dependent Depletion (CADD) scoring [17] is an important
143 bioinformatics filtering method. We compare MRF to the PHRED-scaled *RAG1*
144 CADD scores for all possible SNVs (Fig 5). While CADD is a valuable scoring
145 method its purpose is not to predict likelihood of variation.

146 Discussion

147 Determining disease-causing variants for functional analysis typically aims to
148 target conserved gene regions. On GnomAD 55.99% of *RAG1* (approx. 246,000
149 alleles) has no reported variants. Functionally validating unknown variants in
150 genes with this level purifying selection is generally infeasible. Conserved re-
151 gions are likely high importance regions, yet determining the likelihood of pa-
152 tients presenting with mutations in these clusters requires a scoring mecha-
153 nism. An example of such clustering of highly scoring MRFs occurred in the
154 *RAG1* catalytic RNase H (RNH) domain at p.Ser638-Leu658 which is also con-
155 sidered a conserved *Transib* motif. Targeting clearly defined regions with high
156 MRF scores allows for functional validation studies tailored to the most clinically-
157 relevant protein regions. Phenotypic, epigenetic, or other such weighting data
158 may also be applied to this model. Variants with a low MRF may still be damag-
159 ing but resources for functional validation are best spent on gene regions with
160 high MRF. Table S1 lists the values for calculated MRFs for *RAG1* and *RAG2*.

161 We have presented a basic application of MRF scoring for *RAG* deficiency.
162 Furthermore, we have suggested its genome-wide application with to the infor-
163 mation retrieval method; term frequency, inverse document frequency ($tf -$
164 idf). In this case the “term” will represent an amino acid residue r while the

165 “document” represents a gene g such that,

$$rf - igf_{r,g} = rf_{r,g} \times igf_r \quad (1)$$

166 We may view each gene as a vector with one component corresponding to each
167 residue mutation in the gene, together with a weight for each component that is
168 given by (1). Therefore, we can find the overlap score measure with the $rf - igf$
169 weight of each term in g .

$$\text{Score}(q, g) = \sum_{r \in q} rf \cdot igf_{r,g}.$$

170 We expand here briefly on the technical description of this method. Log weight-
171 ing may offer clearer disease-causing variant discovery depending on the scor-
172 ing method. In respect to MRF scoring, this information retrieval method might
173 be applied as follows; the $rf - igf$ weight of a term is the product of its rf
174 weight and its igf weight ($W_{r,g} = rf_{r,g} \times \log \frac{N}{gf_r}$) or ($W_{r,g} = (1 + \log rf_{r,g}) \times$
175 $\log \frac{N}{gf_r}$). That is, firstly, the number of times a residue mutates in a gene ($rf =$
176 $rf_{r,g}$). Secondly, the rarity of the mutation genome-wide in N number of genes
177 ($igf = N/gf_r$). Finally, ranking the score of genes for a mutation query q by;

$$\text{Score}(q, g) = \sum_{r \in q \cap g} rf \cdot igf_{r,g}$$

178 The score of the query ($\text{Score}(q, g)$) equals the mutations (terms) that appear
179 in both the query and the gene ($r \in q \cap g$). Working out the $rf - igf$ weight for
180 each of those variants ($rf \cdot igf_{r,g}$) and then summing them (Σ) to give the score
181 for the specific gene with respect to the query.

182 During clinical investigations using personalised analysis of patient data,
183 further scoring methods may be applied based on disease features. A patient

184 with autoinflammatory features may require weighting for genes such as *MEFV*
185 and *TNFAIP3*, whereas a patient with mainly immunodeficiency may have weighted
186 scoring for genes such as *BTK* and *DOCK8*. A patient phenotype can contribute
187 a weight based on known genotype correlations separating primary immunod-
188 efficiencies or autoinflammatory diseases [6]. However, validation of these ex-
189 panded implementations requires a deeper consolidation of functional stud-
190 ies than is currently available. A method with similar possible applications for
191 human health mapping constrained coding regions has been recently released
192 [18]. This study employed a method which included weighting by sequencing
193 depth. We have not included this method as our analysis was gene-specific but
194 implementation is advised when calculating genome-wide MRF scores.

195 Predicting the likelihood of discovering novel mutations has implications
196 in genome-wide association studies (GWAS). Variants with low minor allele fre-
197 quencies have a low discovery rate and low probability of disease association
198 [19]; an important consideration for rare diseases such as RAG deficiency. An
199 analysis of the NHGRI-EBI catalogue data highlighted diseases whose average
200 risk allele frequency was low. Autoimmune diseases had risk allele frequen-
201 cies considered low at approximately 0.4 [19]. Without a method to rank most
202 probable novel disease-causing variants, it is unlikely that GWAS will identify
203 very rare disease alleles (with frequencies <0.001). It is conceivable that a num-
204 ber of rare immune diseases are attributable to polygenic rare variants. How-
205 ever, evidence for low-frequency polygenic compounding mutations will not be
206 available until large, accessible genetics databases are available, exemplified by
207 the NIHR BioResource Rare Diseases study [14]. An interesting consideration

208 when predicting probabilities of variant frequency, is that of protective muta-
209 tions. Disease risk variants are quelled at low frequency by negative selection,
210 while protective variants may drift at higher allele frequencies [20].

211 The cost-effectiveness of genomic diagnostic tests is already outperforming
212 traditional, targeted sequencing [1]. Even with substantial increases in data
213 sharing capabilities and adoption of clinical genomics, rare diseases due to
214 variants of unknown significance and low allele frequencies (<0.0001) will re-
215 main non-actionable until reliable predictive genomics practices are developed.
216 Bioinformatics a a whole has made staggering advances in the field of genet-
217 ics [21]. Challenges which remain unsolved, hindering the benefit of national
218 or global genomics databases, include DNA data storage and random access
219 retrieval [22], data privacy management [23], and predictive genomics analy-
220 sis methods. Variant filtration in rare disease is based on reference allele fre-
221 quency, yet the result is not clinically actionable in most cases. Development of
222 predictive genomics tools may provide a critical role for single patient studies
223 and timely diagnosis [13].

224 **Conclusion**

225 We provide the amino acid residue list for RAG1 and RAG2 which have not been
226 reported to date but are most likely to present clinically as RAG deficiency. This
227 method may be applied to other diseases with hopes of improving prepared-
228 ness for clinical diagnosis.

229 **Methods**

230 *Population genetics*

231 GnomAD (version r2.0.2) [24] was queried for the canonical transcripts of *RAG1*
232 and *RAG2* from population genetics data of approximately 146,000 alleles;
233 ENST00000299440 (*RAG1*) 1495 variants (including filtered: 1586),
234 GRCh37 11:36532259-36614706 and ENST00000311485 (*RAG2*) 786 variants (in-
235 cluding filtered: 831), GRCh37 11:36597124 - 36619829. Data was filtered to
236 contain the identifiers: frameshift, inframe deletion, inframe insertion, mis-
237 sense, stop lost, or stop gained. Reference transcripts were sourced from En-
238sembl in the FASTA format amino acid sequence; transcript: RAG1-201
239 ENST00000299440.5 [HGNC:9831] and transcript: RAG2-201 ENST00000311485.7
240 [HGNC:9832]. These sequences were converted to their three-letter code for-
241 mat using One to Three from the Sequence Manipulation Suite
242 (<http://bioinformatics.org/sms2/mirror.html>).

243 Input sets used GnomAD variant allele frequencies and reference sequences
244 processed as cvs files, cleaned and sorted to contain only coding amino acid
245 residues, amino acid code, residue number, alternate variants, allele frequen-
246 cies of variants, and a score (*C*) of 0 or 1 where 1 represented no reported
247 variants. A score was also given where multiple alternate variants existed. A
248 separate statistics report was generated from this processed input data. The
249 percentage of conserved residues was calculated (55.99% of amino acids con-
250 tained no reported variants in *RAG1*, 55.98% in *RAG2*). The count of variants
251 per residue was found for both proteins. The ratio was also found per residue

252 conservation rate / mutation rate. Basic protein statistics were generated using
253 reference canonical transcript sequences of RAG1 and RAG2 with the Sequence
254 Manipulation Suite. The residue frequency was calculated based on the respec-
255 tive polypeptide chain length.

256 The calculated mutation rate value and residue frequency score together
257 produce the mutation rate residue frequency as shown in Table S1. Our inves-
258 tigation used the Boolean *C* score of 0 or 1 to weight mutation rate residue fre-
259 quencies. An important consideration for future application is whether to use
260 this Boolean score or a frequency score. In the clinical setting, the likelihood of
261 *de novo* mutations versus inherited mutations have different impact on reces-
262 sive and dominant diseases. The likelihood of a patient presenting with a par-
263 ticular (predicted) variant is more likely if the variant exists even at a very low
264 frequency in the patients ancestral population. Therefore, an allele frequency
265 may be used to replace *C* in many investigations.

266 *Data visualisation*

267 For our visualisation of MRF scores, small clusters of high MRF were of more
268 significance than individual highly conserved residues. Therefore, we applied a
269 1% average filter where values were averaged over a sliding window of *N* num-
270 ber of residues (10 in the case of RAG1, 6 in the case of RAG2). However, when
271 using Boolean scoring *C*, this method should be applied before *C*. Alternatively,
272 if using allele frequency scoring, this visualisation method can be applied sub-
273 sequently. Lastly, for a clear distinction of MRF clusters a cut-off threshold was
274 applied at the 75th percentile (0.0168 in RAG1).

275 A gene map for coding regions in RAG1 and RAG2 were populated with (1)
276 Boolean *C* score from population genetics data, (2) raw MRF scores, and (3)
277 MRF clusters with 1% average and cutoff threshold. GraphPad Prism was used
278 for heatmaps and Adobe Adobe Illustrator and Photoshop were used for protein
279 domain illustrations.

280 *Validation of MRF against functional data*

281 The recombination activity of RAG1 and RAG2 was previously measured on 44
282 known pathogenic variants [14, 15]. Briefly, the pathogenicity of variants in
283 RAG1 and RAG2 are measured functionally *in vitro* by expression of RAG1 and
284 RAG2 in combination with a recombination substrate plasmid containing re-
285 combination signal sequences which are targeted by RAG complex during nor-
286 mal V(D)J recombination. Recombination events are assessed by quantitative
287 real-time PCR using comparative CT. The inverse score of recombination activ-
288 ity (0-100%) is used to quantify pathogenicity of variants in our study. Compar-
289 ison between known pathogenicity scores and MFR was done by scaling MRF
290 scores from 0-100% (100% being highest probability of occurring as damaging).

291 **References**

- 292 [1] Katherine Payne, Sean P Gavan, Stuart J Wright, and Alexander J Thomp-
293 son. Cost-effectiveness analyses of genetic and genomic diagnostic tests.
294 *Nature Reviews Genetics*, 2018.
- 295 [2] Antonia Kwan, Roshini S Abraham, Robert Currier, Amy Brower, Karen An-
296 druszewski, Jordan K Abbott, Mei Baker, Mark Ballow, Louis E Bartoshesky,

- 297 Vincent R Bonagura, et al. Newborn screening for severe combined im-
298 munodeficiency in 11 screening programs in the united states. *Jama*, 312
299 (7):729–738, 2014.
- 300 [3] L. Alexander Liggett, Anchal Sharma, Subhajyoti De, and James DeGre-
301 gori. Conserved patterns of somatic mutations in human peripheral blood
302 cells. *bioRxiv*, 2017. doi: 10.1101/208066.
- 303 [4] Kapourani Chantriolnt-Andreas Stubbs Thomas M. Lee Heather J. Alda-
304 Catalinas Celia Krueger Felix Sanguinetti Guido Kelsey Gavin Marioni John
305 C. Stegle Oliver Reik Wolf Clark Stephen J., Argelaguet Ricard. scnm-
306 seq enables joint profiling of chromatin accessibility dna methylation and
307 transcription in single cells. *Nature Communications*, 9(1):781, 2018. ISSN
308 2041-1723. doi: 10.1038/s41467-018-03149-4.
- 309 [5] István Bartha, Julia di Iulio, J Craig Venter, and Amalio Telenti. Human
310 gene essentiality. *Nature Reviews Genetics*, pages nrg–2017, 2017.
- 311 [6] Capucine Picard, Waleed Al-Herz, Aziz Bousfiha, Jean-Laurent Casanova,
312 Talal Chatila, Mary Ellen Conley, Charlotte Cunningham-Rundles, Amos
313 Etzioni, Steven M Holland, Christoph Klein, et al. Primary immunode-
314 ficiency diseases: an update on the classification from the international
315 union of immunological societies expert committee for primary immu-
316 nodeficiency 2015. *Journal of clinical immunology*, 35(8):696–726, 2015.
- 317 [7] Mary Ellen Conley and Jean-Laurent Casanova. Discovery of single-gene

- 318 inborn errors of immunity by next generation sequencing. *Current opin-*
319 *ion in immunology*, 30:17–23, 2014.
- 320 [8] David G Schatz, Marjorie A Oettinger, and David Baltimore. The v (d) j
321 recombination activating gene, rag-1. *Cell*, 59(6):1035–1048, 1989.
- 322 [9] Marjorie A Oettinger, David G Schatz, Carolyn Gorka, and David Balti-
323 more. Rag-1 and rag-2, adjacent genes that synergistically activate v (d)
324 j recombination. *Science*, 248(4962):1517–1523, 1990.
- 325 [10] Jolan E Walter, Lindsey B Rosen, Krisztian Csomos, Jacob M Rosenberg,
326 Divij Mathew, Marton Keszei, Boglarka Ujhazi, Karin Chen, Yu Nee Lee,
327 Irit Tirosh, et al. Broad-spectrum antibodies against self-antigens and cy-
328 tokines in rag deficiency. *The Journal of clinical investigation*, 125(11):
329 4135–4148, 2015.
- 330 [11] Catharina Schuetz, Kirsten Huck, Sonja Gudowius, Mosaad Megahed,
331 Oliver Feyen, Bernd Hubner, Dominik T Schneider, Burkhard Manfras, Ul-
332 rich Pannicke, Rein Willemze, et al. An immunodeficiency disease with
333 rag mutations and granulomas. *New England Journal of Medicine*, 358(19):
334 2030–2038, 2008.
- 335 [12] Tami John, Jolan E Walter, Catherina Schuetz, Karin Chen, Roshini S Abra-
336 ham, Carmem Bonfim, Thomas G Boyce, Avni Y Joshi, Elizabeth Kang,
337 Beatriz Tavares Costa Carvalho, et al. Unrelated hematopoietic cell trans-
338 plantation in a patient with combined immunodeficiency with granulo-

- 339 matous disease and autoimmunity secondary to rag deficiency. *Journal of*
340 *clinical immunology*, 36(7):725–732, 2016.
- 341 [13] Jean-Laurent Casanova, Mary Ellen Conley, Stephen J Seligman, Laurent
342 Abel, and Luigi D Notarangelo. Guidelines for genetic studies in single pa-
343 tients: lessons from primary immunodeficiencies. *Journal of Experimen-*
344 *tal Medicine*, pages jem–20140520, 2014.
- 345 [14] Dylan Lawless, Christoph B Geier, Jocelyn R Farmer, Hana Allen Lango,
346 Daniel Thwaites, Faranaz Atschekzei, Matthew Brown, David Buchbinder,
347 Siobhan O Burns, Manish J Butte, et al. Prevalence and clinical chal-
348 lenges among adult primary immunodeficiency patients with rag defi-
349 ciency. *Journal of Allergy and Clinical Immunology*.
- 350 [15] Yu Nee Lee, Francesco Frugoni, Kerry Dobbs, Irit Tirosh, Likun Du,
351 Francesca A Ververs, Heng Ru, Lisa Ott de Bruin, Mehdi Adeli, Jacob H
352 Bleesing, et al. Characterization of t and b cell repertoire diversity in pa-
353 tients with rag deficiency. *Science immunology*, 1(6), 2016.
- 354 [16] Vladimir V Kapitonov and Jerzy Jurka. Rag1 core and v (d) j recombination
355 signal sequences were derived from transib transposons. *PLoS biology*, 3
356 (6):e181, 2005.
- 357 [17] Martin Kircher, Daniela M Witten, Preti Jain, Brian J O’roak, Gregory M
358 Cooper, and Jay Shendure. A general framework for estimating the relative
359 pathogenicity of human genetic variants. *Nature genetics*, 46(3):310, 2014.

- 360 [18] James M Havrilla, Brent S Pedersen, Ryan M Layer, and Aaron R Quinlan. A
361 map of constrained coding regions in the human genome. *bioRxiv*, 2017.
362 doi: 10.1101/220814.
- 363 [19] Takashi Kido, Weronika Sikora-Wohlfeld, Minae Kawashima, Shinichi
364 Kikuchi, Naoyuki Kamatani, Anil Patwardhan, Richard Chen, Marina
365 Sirota, Keiichi Kodama, Dexter Hadley, et al. Are minor alleles more likely
366 to be risk alleles? *BMC medical genomics*, 11(1):3, 2018.
- 367 [20] Yingleong Chan, Elaine T Lim, Niina Sandholm, Sophie R Wang,
368 Amy Jayne McKnight, Stephan Ripke, Mark J Daly, Benjamin M Neale,
369 Rany M Salem, Joel N Hirschhorn, et al. An excess of risk-increasing low-
370 frequency variants can be a signal of polygenic inheritance in complex dis-
371 eases. *The American Journal of Human Genetics*, 94(3):437–452, 2014.
- 372 [21] Maxwell W Libbrecht and William Stafford Noble. Machine learning ap-
373 plications in genetics and genomics. *Nature Reviews Genetics*, 16(6):321,
374 2015.
- 375 [22] Lee Organick, Siena Dumas Ang, Yuan-Jyue Chen, Randolph Lopez, Sergey
376 Yekhanin, Konstantin Makarychev, Miklos Z. Racz, Govinda Kamath,
377 Parikshit Gopalan, Bichlien Nguyen, Christopher Takahashi, Sharon New-
378 man, Hsing-Yeh Parker, Cyrus Rashtchian, Kendall Stewart, Gagan Gupta,
379 Robert Carlson, John Mulligan, Douglas Carmean, Georg Seelig, Luis Ceze,
380 and Karin Strauss. Scaling up dna data storage and random access re-
381 trieval. *bioRxiv*, 2017. doi: 10.1101/114553.

- 382 [23] Zhicong Huang, Erman Ayday, Huang Lin, Raeka S. Aiyar, Adam
383 Molyneaux, Zhenyu Xu, Jacques Fellay, Lars M. Steinmetz, and Jean-Pierre
384 Hubaux. A privacy-preserving solution for compressed storage and se-
385 lective retrieval of genomic data. *Genome Research*, 26(12):10. 1687–1696,
386 2016.
- 387 [24] Monkol Lek, Konrad J Karczewski, Eric V Minikel, Kaitlin E Samocha, Eric
388 Banks, Timothy Fennell, Anne H O’Donnell-Luria, James S Ware, An-
389 drew J Hill, Beryl B Cummings, et al. Analysis of protein-coding genetic
390 variation in 60,706 humans. *Nature*, 536(7616):285, 2016.

Table S1: MRF data tables. The complete RAG1 and RAG2 amino acid residue MRF scores are provided along with known clinically pathogenic variant residues and raw data used for calculations.

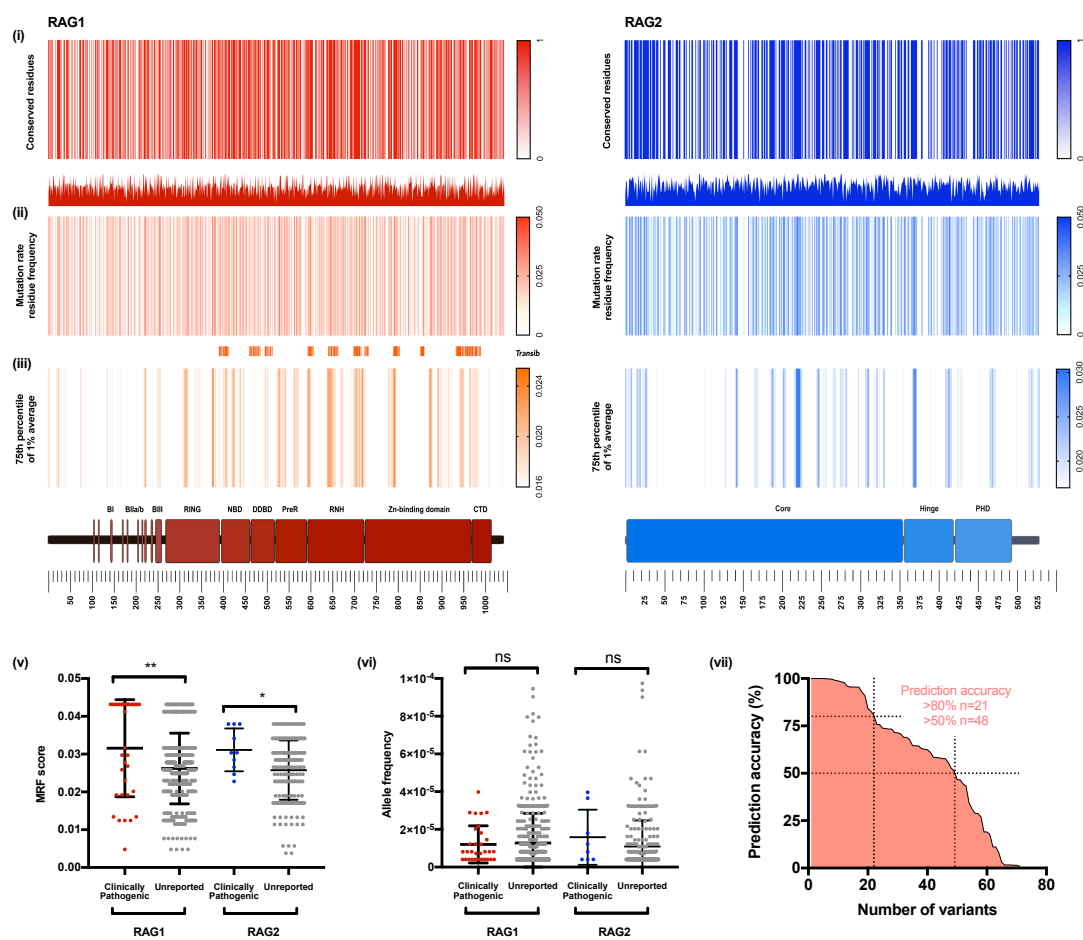


Figure 1: RAG1 and RAG2 conservation and mutation rate residue frequency. (i) Gene conservation score, non-conserved 0 and conserved 1. (ii) Histogram; raw MRF score. Heatmap; MRF prediction for conserved residues, graded 0 to 0.05. (iii) MRF score averaged with 1% intervals for each respective gene and cut-off below 75th percentile, graded 0 to 0.03 (Noise reduction method). (iv) Gene structure with functional domains. (v) Clinically damaging variants reported on GnomAD have significantly higher MRF scores than non-pathogenic variants. (Unpaired t test. RAG1 P value 0.002** RAG2 P value 0.0339*). (vi) GnomAD allele frequency <0.0001. No significant difference in allele frequency is found between clinically damaging variants and non-clinically reported. (vi) Accuracy of MRF scoring compared to functionally validated pathogenicity.

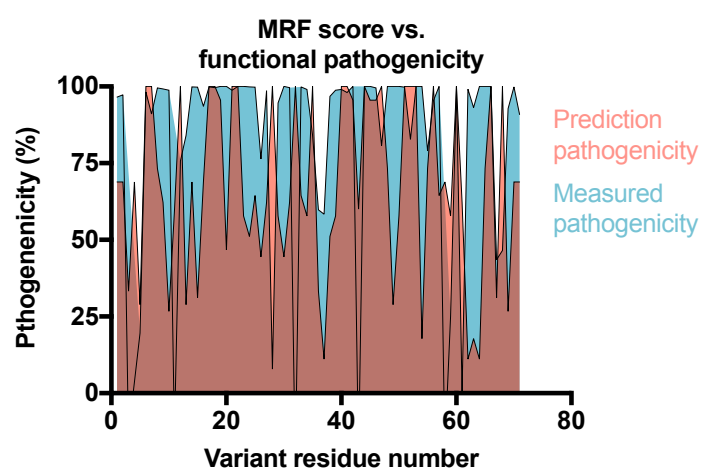


Figure 2: MRF score vs. known variant pathogenicity measure. Predicted pathogenicity likelihood (based on maximum and minimum MRF score as a percentage) is shown in red. In blue, the functionally measured recombination activity of each variant where complete loss of protein activity is measured as 100% pathogenicity. These values are summarised in Fig 1v(ii).

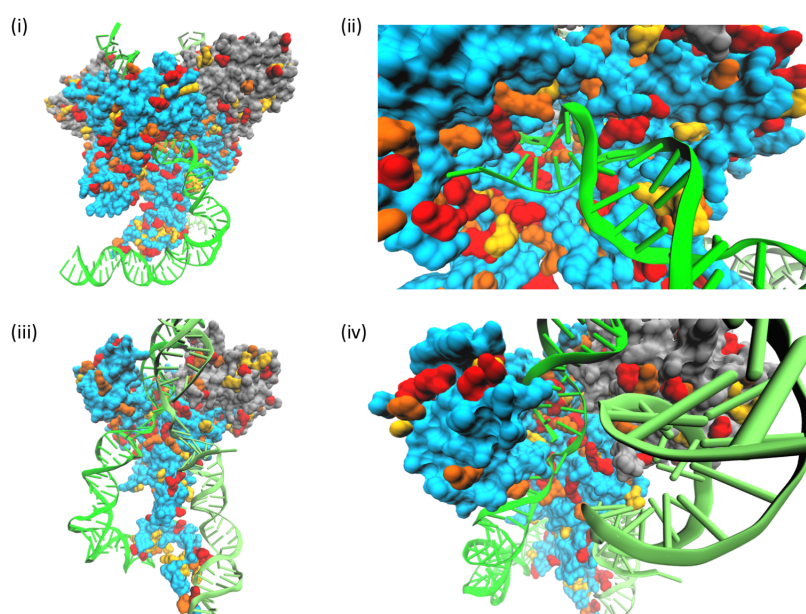


Figure 3: The RAG1 (blue) and RAG2 (grey) protein structure with MRF scores. (i) Protein dimers and (ii-iv) monomers illustrating the three highest category MRF scores for predicted clinically-relevant variants. Increasing in MRF score; yellow, orange, red. DNA contact points are integral to protein function and generally score as high MRF residues. (PDB:3jbw)

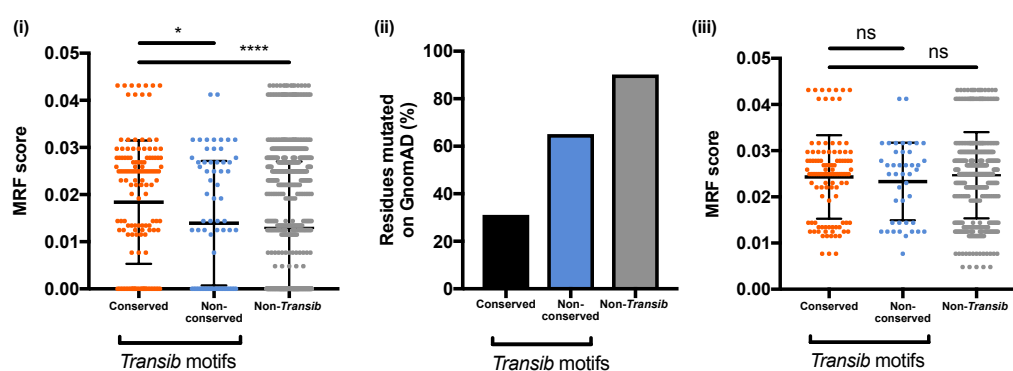


Figure 4: False positives in *Transib* domains do not worsen probability prediction. The *Transib* domains contain critical conserved protein residues. (i) False positives are simulated by scoring *Transib* domains MRF without their Boolean conservation weight *C*. (ii) Allele frequencies on GnomAD have inversely proportional conservation to simulated false-positive MRF scoring. (iii) When the Boolean component *C* is applied in MRF calculation the effect of false positives remains non-significant, illustrating the non-negative impact of MRF for pathogenicity rate prediction.

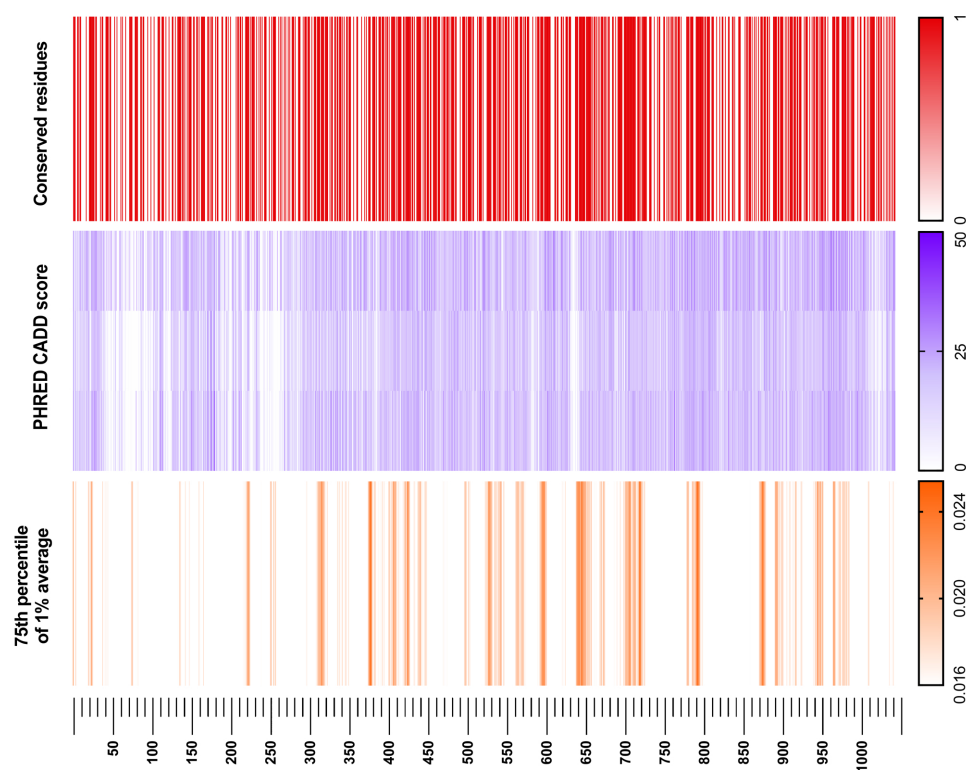


Figure 5: *RAG1* PHRED-scaled CADD score versus GnomAD conservation rate and MRF score. Allele frequency conservation rate (top) is vastly important for identifying critical structural and functional protein regions. The impact of mutation in one of these conserved regions is often estimated using CADD scoring (middle). The MRF score (bottom)(visualised using the 75th percentile with 1% averaging) highlights protein regions which are most likely to present clinically and may require pre-emptive functional investigation.